

## **Design and Characteristics of Directional Coupler Based Filters**

**R. T. Balat<sup>\*</sup>, M. F. O. Hameed<sup>\*</sup>, S. S. A. Obayya<sup>\*\*</sup>, M. I. Abo el Maaty<sup>\*</sup>,  
M. M. Abo-Elkhier<sup>\*</sup>, and H. A. El-Mikati<sup>\*\*\*</sup>**

<sup>\*</sup>Department of Mathematics and Engineering Physics, Faculty of Engineering, Mansoura University, Mansoura 35516, Egypt.

<sup>\*\*</sup>Director of Centre for Photonics and Smart Materials, Zewail City of Science and Technology, Sheikh Zayed District, 6th of October City, Giza, Egypt.

<sup>\*\*\*</sup>Department of Electronics and Communications Engineering, Faculty of Engineering, Mansoura University, Mansoura 35516 Egypt.

### **ABSTRACT**

In this paper, an accurate characterization of a novel design of an optical wavelength filter is investigated and analyzed by the coupled mode theory (CMT). The effect of the different structure geometrical parameters on the filter performance is studied. The crosstalk and bandwidth of the device are also calculated for various separations between the waveguides. The suggested design has a crosstalk of -34.909 dB and bandwidth of 14.8 nm for device length of 1646.26  $\mu\text{m}$ . A bandwidth of 10 nm can also be obtained with a device length of 3.1 mm. In addition, a novel design of cascaded structure of non-identical directional coupler is introduced and analyzed by the CMT. The suggested design offers complete power exchange between two slab waveguides having modes with different propagation constants. The reported coupler exhibits low crosstalk of -38.38dB with a compact device length of 171.54 $\mu\text{m}$ .

**Keywords - coupled mode analysis, directional couplers, optical filters**

### **1. INTRODUCTION**

The increase of the channel information capacity represents an important issue in the optical communication systems. The narrow bandwidth (BW) optical filters are the key devices for a wavelength division multiplexing (WDM) and demultiplexing to combine and separate wavelengths carrying different information and thus can be used to increase the transmission capacity of the existing fiber link.

The capability of transferring power between waveguides is a key function for many applications of integrated optics. The directional coupler is ideal for designing many important optical devices such as optical switches, modulators, power divider and filters [1-6]. The directional couplers, consisting of a pair of closely spaced, single-mode, parallel slab waveguides, may be used as filters [7,8].

A large tuning range is expected and fabrication is rather easy. However, the reported bandwidth of the conventional directional coupler is more than 5 nm.

During the last few years, various accurate modelling methods have been developed for modal analysis of different waveguides. These methods included the finite difference method [9], finite element method [10] and beam propagation method (BPM) [11]. The numerical modal solution techniques are mostly accurate and able to deal with many complex structures. However, this accuracy results in an algorithm that is complex to implement. In addition, these methods are time consuming since they rely on fine meshes for an acceptable accuracy. On the contrary the analysis based on coupled mode theory (CMT) [12,13] is very attractive because of its simple implementation.

In this paper, a rigorous characterization of an optical wavelength filter is investigated through the (CMT) [12]. The filter structure is simply a conventional directional coupler of two non-identical uniform dielectric slab waveguides. Each waveguide propagates only the fundamental transverse electric (TE) mode. In addition, the guiding media are isotropic, linear, and lossless. Hardy and Streifer published several papers [14] in which coupled mode theory was derived for parallel dielectric waveguides that may contain loss or gain. Haus et al [13] then utilized a variational principle (VP) for the lossless case, obtaining similar equations which are compared with those obtained in [14]. The reported results by Hardy and Streifer [14] and Haus et al. [13] clarify that the results for waveguides that may contain loss or gain are identical to those obtained for lossless guiding media for the transverse electric (TE) modes and differ negligibly for transverse magnetic (TM) modes [15].

The directional couplers that made of uniform waveguides can couple light between waveguides only when the waveguides modes are phase matched. This means for single mode waveguides that the two waveguides have to be identical. In this study, the reported structure consists of two non-identical slab waveguides of different widths  $W_1$  and  $W_2$  which are separated by a distance of  $2s$ . The waveguides modes are initially not phase matched with different propagation constants. Then, the widths of the two waveguides are chosen to achieve the phase matching condition with index

discontinuity of order  $10^{-7}$ . The coupling length at which the maximum power transfer occurs is calculated. In addition, the filter response, crosstalk and bandwidth are reported as a function of the operating wavelength. Moreover, the effects of the structure geometrical parameters on the filter response, crosstalk, and bandwidth are introduced. The suggested design has a crosstalk of -34.909 dB and bandwidth of 14.8 nm with a device length of 1646.26  $\mu\text{m}$ . A bandwidth of 10 nm can also be achieved for a device length of 3.1 mm. The numerical results obtained by the CMT are validated by those obtained by the BPM and an excellent agreement is achieved. In addition, the CMT is simple for implementation and overcomes the computation time problem of the other modelling method.

It has been noticed that complete exchange of light power between the two waveguides occurs when their modes are initially phase matched. In addition, a slightly difference in the waveguides widths  $W_1$  or  $W_2$  will decrease the coupling efficiency and the peak value of the output power will be shifted from the operating wavelength  $\lambda=1.3\mu\text{m}$ . This means that the phase matching between the waveguides modes is no longer achieved. It is also found that, if the waveguides modes have different propagation constants and the widths of the two waveguides do not realize the matching condition, the coupling efficiency can be increased if the separation between the waveguides decreased, however, the separation between the waveguides cannot be too small. To overcome these limitations, a novel design of cascaded non-identical directional coupler is introduced and analyzed. The reported structure achieves complete power transfer even if the waveguides modes are originally not phase matched. The numerical results reveal that complete power exchange between the two waveguides is achieved with low crosstalk of -38.38 dB. In addition, the cascaded structure has a compact device length of 171.54  $\mu\text{m}$  which is much shorter than any reported length of uniform directional coupler at this crosstalk value. The analysis is based on the coupled mode formalism [12], with the transfer-matrix method (TMM) [16] as a general solution technique. The numerical results obtained by the CMT are validated by those obtained by the BPM and an excellent agreement is achieved.

The paper is organized as follows: The mathematical formulation of uniform directional coupler is introduced in section 2. A numerical simulation for the two proposed designs and discussion of their results are presented in section 3 and 4. Finally conclusions are drawn in section 5.

## 2. Mathematical Formulation

The structure of the uniform directional coupler consists of two individual slab waveguides placed in close proximity. These slab waveguides are

parallel to each other as shown in Fig. 1. Each waveguide propagates only the fundamental TE mode with implicit time dependence  $\exp(j\omega t)$ , where,  $\omega$  represents the angular frequency  $\omega=2\pi f$ . The amplitudes of these modes are denoted by  $a_1$  and  $a_2$ . These waveguide modes will propagate independently with their propagation constants  $\beta_1$  and  $\beta_2$ .

The modes associated with each individual waveguide being perturbed by the presence of the others. These perturbations lead to coupling and exchange of power among the guided modes. The amplitudes of the composite modes are governed by the coupled-mode equations which will be solved analytically by the transfer matrix method (TMM) [16]. The solutions of the coupled mode equations describe wave propagation and coupling in the coupled-waveguide system.

The coupled equations of the spatial dependences of one mode amplitude should be of the form [12]

$$\frac{da_1}{dz} = -j(\beta_1 + k_{11})a_1 - jk_{12}a_2 \quad (1-a)$$

$$\frac{da_2}{dz} = -j(\beta_2 + k_{22})a_2 - jk_{21}a_1 \quad (1-b)$$

where  $k_{ii}$  represents the self coupling coefficients and  $k_{ij}$  represents the mutual coupling coefficients. The trial solution is expressed as linear superposition of waveguide modes.

$$E = \sum a_i(z) e_i(x, y) = a_1(z)e_1 + a_2(z)e_2 \quad (2-a)$$

$$H = \sum a_i(z) h_i(x, y) = a_1(z)h_1 + a_2(z)h_2 \quad (2-b)$$

where,  $e_i$  and  $h_i$  are the normalized solutions of the electric and magnetic fields, respectively. In addition,  $a_1$  and  $a_2$  represent the corresponding waveguide mode amplitudes. Moreover,  $E$  and  $H$  represent the electric and magnetic fields of the composite modes. The coupled mode equations are [12]

$$P \frac{d}{dz} A = -j H A \quad (3)$$

where

$$H_{ij} = P_{ij} \beta_j + K_{ij} \quad (4)$$

$$P_{ij} = \frac{1}{4} \int [e_j \times h_i^* + e_i^* \times h_j] \cdot z' da$$

$$K_{ij} = \frac{1}{4} \omega \epsilon_0 \int (n^2 - n_j^2) e_i^* \cdot e_j da$$

where  $P_{ij}$  is the power matrix element,  $K_{ij}$  is the coupling coefficients for the natural coupling between the two waveguides,  $n$  is the actual refractive index distribution of the uniform coupler, and  $n_j$  is the index of the  $j^{\text{th}}$  waveguide in the absence of the other waveguides. After some mathematical treatments and solving the coupled mode (CM)

equations the mode amplitudes may be expressed in terms of the transfer matrix (TM) as:

$$A(z) = T(z) A(0) \quad (5)$$

and the guided power will be calculated from

$$P_1(z) = |a_1(z)|^2 \quad (6)$$

$$P_2(z) = |a_2(z)|^2 \quad (7)$$

In this study the coupling length ( $L_c$ ) defined as the length at which the maximum power transfer from one waveguide to the other occurs, is calculated from

$$L_C = \frac{\pi}{\beta_s - \beta_a} \quad (8)$$

where  $\beta_s$  and  $\beta_a$  are the propagation constants of symmetric and asymmetric composite modes, respectively.

### 3. Numerical Results

Figure 1 shows a schematic diagram of the proposed design of an optical wavelength filter. The structure consists of two parallel dielectric waveguides of widths  $W_1$  and  $W_2$  with refractive indices  $n_1$  and  $n_2$ , respectively. The two layers are placed parallel to each other with a separation layer of width  $2s$  and refractive index  $n_c$ . The waveguides of the proposed design consist of  $\text{In}_{1-x}\text{Ga}_x\text{As}_y\text{P}_{1-y}$  material, for the guiding layers, with arsenic fractions ( $y$ ) of 0.25 for the first waveguide and 0.15 for the second waveguide. In addition, InP material is used for the cladding and separation layers with  $x=y=0$ . The relation between  $x$  and  $y$  for lattice matching is obtained from [17].

$$x = \frac{0.1894 y}{(0.4184 - 0.013 y)} \quad (9)$$

where  $x$  represents the Ga content at lattice matching. The refractive indexes  $n_1$  and  $n_2$  for the two guiding layers, and the refractive index of InP in the cladding and separation layers  $n_c$  are calculated by using the formulas [17,18]:

$$n(\lambda) = \left[ 1 + \frac{E_d}{E_0} + \frac{E_d E^2}{E_0^3} + \frac{\eta E^4}{\pi} \ln \left( \frac{2E_0^2 - E_g^2 - E^2}{E_g^2 - E^2} \right) \right]^{1/2} \quad (10)$$

where

$$\eta = \frac{\pi E_d}{2E_0^3 (E_0^2 - E_g^2)} \quad (10.a)$$

$$E_0 = 0.595 x^2 (1 - y) + 1.626 xy - 1.891 y + 0.524 x + 3.391 \quad (10.b)$$

$$E_d = (12.36x - 12.71)y + 7.54x + 28.91 \quad (10.c)$$

$$E_g [\text{ev}] = 1.35 - 0.72y + 0.12y^2 \quad (10.d)$$

$$E = \frac{1.24}{\lambda(\mu\text{m})} \quad (10.e)$$

The InGaAsP/InP semiconductor material has wavelength-dependent index variation, and possible electronic tuning. Therefore, the filter bandwidth and the center frequency can be designed by controlling the waveguide parameters and the material composition of GaInAsP during the epitaxial growth. The wavelength dependent refractive indexes  $n_1$  and  $n_2$  for the two guiding layers, when lattice matched to InP at fixed  $x$  and  $y$  values are shown in Fig. 2. The variation of the refractive index  $n_c$  of InP in the cladding and separation regions with the wavelength is also shown in Fig. 2. It is revealed from this figure that the refractive indexes  $n_1$  and  $n_2$  of the guiding layers and that of the substrate and cladding layers  $n_c$  decrease with increasing the wavelength.

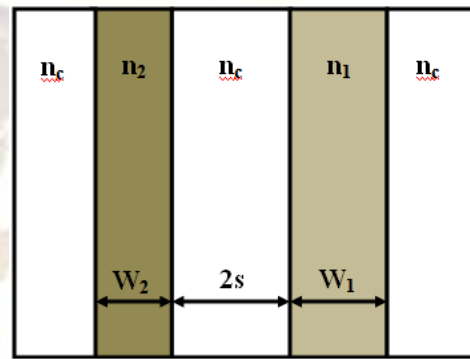


Figure 1 Schematic diagram of an optical wavelength filter

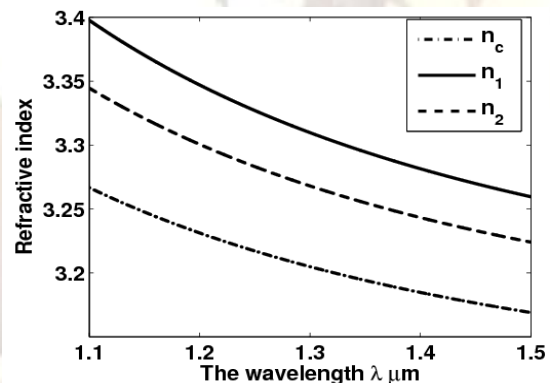


Figure 2 Variation of refractive index with the wavelength.

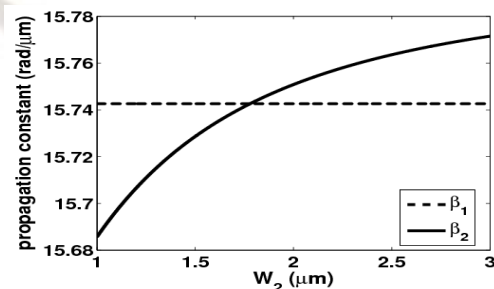


Figure 3 Variation of propagation constants of the two waveguide modes with  $W_2$ .

In this study, the width of the first waveguide  $W_1$  and the separation between the two waveguides  $2s$  are taken as  $0.55 \mu\text{m}$ , and  $1.47 \mu\text{m}$ , respectively. In addition,  $n_1$ ,  $n_2$ , and  $n_c$  are fixed to 3.30970, 3.26799, and 3.20483, respectively [19-21] at the operating wavelength of  $1.3 \mu\text{m}$ . The width of the second waveguide  $W_2$  is chosen so that the matching condition is satisfied. The propagation constants  $\beta_1$  and  $\beta_2$  of the waveguides TE modes are evaluated for different  $W_2$  values as shown in Fig. 3. It is evident from this figure that the matching condition occurs when  $W_2$  is equal to  $1.78 \mu\text{m}$  at which the index discontinuity, defined as the difference between the effective refractive indices of the waveguides modes, will be very small ( $\Delta n = |n_{\text{eff}1} - n_{\text{eff}2}| = 2.707e^{-7}$ ).

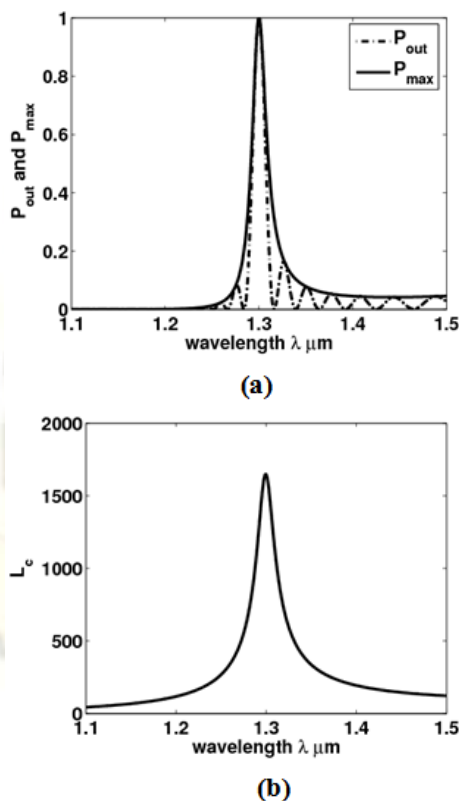


Figure 4 Variation of independent wavelength (a) output and maximum power and (b) the coupling length

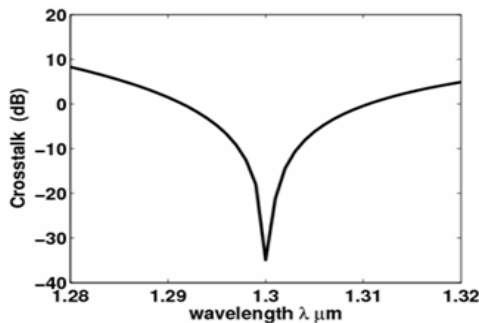


Figure 5 Variation of the crosstalk with the wavelength

The fundamental TE modes at different wavelengths are launched into the first waveguide and the variations of the output power  $P_{\text{out}}$  and the maximum power  $P_{\text{max}}$  as a function of the wavelength are shown in Fig. 4(a). The wavelength dependent coupling length is also shown in Fig. 4(b). It is revealed from Fig.4(a) that the maximum values of  $P_{\text{out}}$  and  $P_{\text{max}}$  are achieved at the phase matching wavelength of  $1.3 \mu\text{m}$ . It is also found that the maximum coupling length of  $1646.26 \mu\text{m}$  is fulfilled at wavelength of  $1.3 \mu\text{m}$ . Moreover,  $L_c$  decreases as the operating wavelength is far from the matching wavelength value. In this case, the variation in the wavelength value has a small effect on  $L_c$  as shown in Fig. 4(b). Figure 5 shows the variation of the crosstalk with the wavelength. In this study, the length of the proposed filter is fixed to  $1646.26 \mu\text{m}$  which is equal to the coupling length at  $\lambda = 1.3 \mu\text{m}$  at which maximum power transfer is achieved. It is revealed from this figure that the crosstalk has a minimum value of  $-34.909 \text{ dB}$  at the operating wavelength  $1.3 \mu\text{m}$ . As the wavelength moves away from the matching wavelength  $1.3 \mu\text{m}$ , the crosstalk is increased.

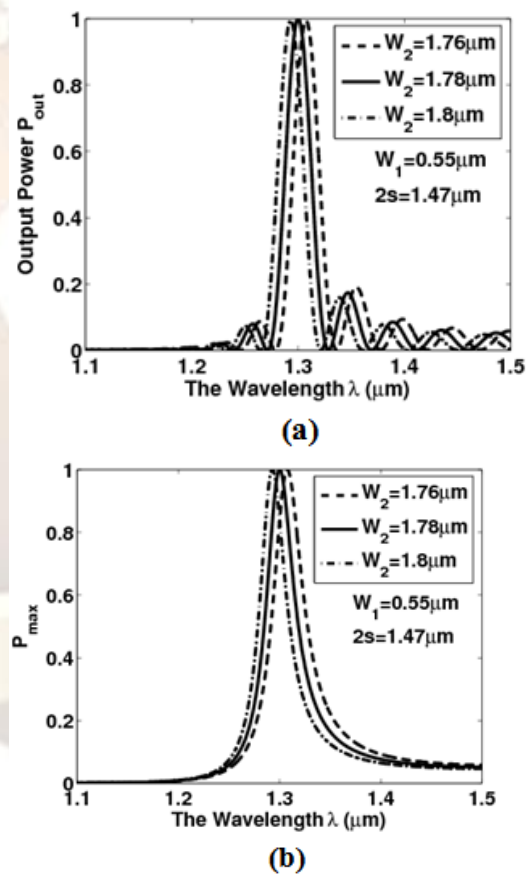


Figure 6 Variation of (a)  $P_{\text{out}}$  and (b)  $P_{\text{max}}$  with the wavelength at different  $W_2$  values

Next, the effects of the structure parameters such as the width of the two waveguides  $W_1$  and  $W_2$  on  $P_{\text{out}}$ ,  $P_{\text{max}}$ , and  $L_c$  are studied. First the effect of  $W_2$

is considered. In this study, all the other structure parameters are fixed to  $n_1=3.30970$ ,  $n_2=3.26799$ ,  $n_c=3.20483$ ,  $W_1=0.55\ \mu\text{m}$ ,  $2s=1.47\ \mu\text{m}$ . Figure 6(a) and (b) show the wavelength dependence of  $P_{\text{out}}$  of the second waveguide and  $P_{\text{max}}$ , respectively for different  $W_2$  values, 1.76, 1.78, and 1.8  $\mu\text{m}$ . It is found that the coupling power efficiency slightly decreases from 0.99998 to 0.996 and 0.9949 as  $W_2$  is varied by  $\pm 0.02\ \mu\text{m}$ , respectively, at a device length of 1646.26  $\mu\text{m}$ . Moreover, the peak value of the output power is shifted from 1.3  $\mu\text{m}$  to 1.296  $\mu\text{m}$  and 1.304  $\mu\text{m}$  as  $W_2$  is varied by  $\pm 0.02\ \mu\text{m}$ , respectively. The effect of  $W_2$  on the  $L_c$  is also studied and reported in Fig.7. It is revealed from this figure that the coupling length decreases as  $W_2$  decreases at the matching wavelength. In addition, the variation in the coupling length becomes insensitive to the variation of  $W_2$  as the wavelength is far from the phase matching wavelength of 1.3  $\mu\text{m}$ .

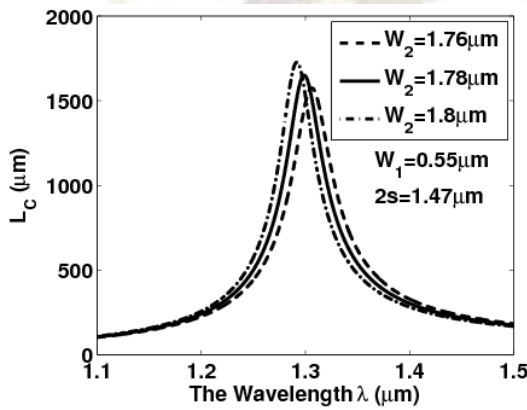
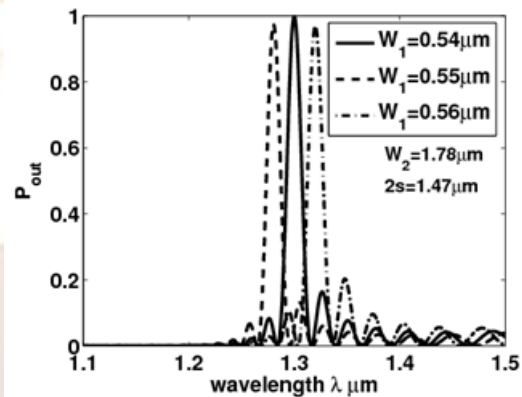


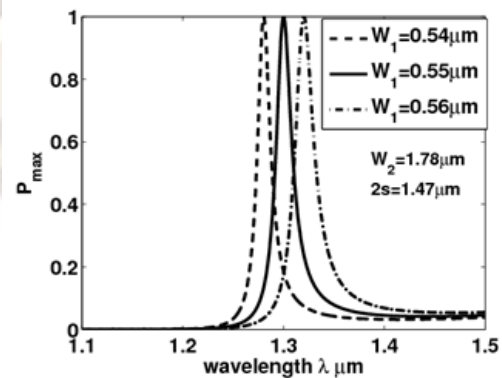
Figure 7 Variation of  $L_c$  with the wavelength at different  $W_2$  values

The effect of  $W_1$  on  $P_{\text{out}}$  of the second waveguide,  $P_{\text{max}}$ , and  $L_c$  is also investigated as shown in Fig. 8(a), Fig. 8(b), and Fig. 9. In this study, the other structure parameters are fixed to  $n_1=3.30970$ ,  $n_2=3.26799$ ,  $n_c=3.20483$ ,  $2s=1.47\ \mu\text{m}$ , and  $W_2=1.78\ \mu\text{m}$ . It is explored that the variation in  $W_1$  value has a much more effect on  $P_{\text{out}}$  and  $P_{\text{max}}$ . If  $W_1$  is varied from 0.55  $\mu\text{m}$  to 0.54 and 0.56  $\mu\text{m}$ , the peak of the maximum and output power will be decreased from 0.99998 to 0.9706 at  $\lambda=1.28\ \mu\text{m}$  and 0.9684 at  $\lambda=1.32\ \mu\text{m}$ , respectively. If the variation of the  $L_c$  is considered, it will be noticed that, if  $W_1$  is changed from 0.55  $\mu\text{m}$  to 0.54 and 0.56  $\mu\text{m}$ , the peak of the coupling length will be 1842.4  $\mu\text{m}$  at  $\lambda=1.2799\ \mu\text{m}$  and 1481.1  $\mu\text{m}$  at  $\lambda=1.3194\ \mu\text{m}$ , respectively. Moreover, as the wavelength is far from the phase matching wavelength the coupling length becomes insensitive to the variation of  $W_1$  as shown in Fig. 9. The effect of the separation  $2s$  between the two waveguides on  $P_{\text{out}}$ ,  $P_{\text{max}}$ ,  $L_c$ , the crosstalk dB, and the bandwidth (BW) is studied. In this evaluation,

$n_1=3.30970$ ,  $n_2=3.26799$ ,  $n_c=3.20483$ ,  $W_2=1.78\ \mu\text{m}$ ,  $W_1=0.55\ \mu\text{m}$ , while,  $2s$  takes different values from 1.47  $\mu\text{m}$  to 1.7  $\mu\text{m}$ . It is revealed from the numerical results that the separation  $2s$  has no noticeable impact on the coupling power efficiency. However, the coupling length increases as the separation between the two waveguides increases. Moreover, if we considered the effect of the variation of the separation on the crosstalk and bandwidth, it is found that the crosstalk decreases as the separation between the waveguides increases. As the separation  $2s$  increases from 1.47  $\mu\text{m}$  to 1.7  $\mu\text{m}$  the crosstalk decreases from -34.9 dB to -39.1662 dB, respectively. In addition, as the separation  $2s$  increases from 1.47  $\mu\text{m}$  to 1.7  $\mu\text{m}$  the bandwidth decreases from 14.8 nm to 10 nm, respectively. However, the coupling length increases from 1646.26  $\mu\text{m}$  to 3.1 mm as the separation  $2s$  increases from 1.47  $\mu\text{m}$  to 1.7  $\mu\text{m}$ , respectively. It can be concluded that the improvement of the filter performance in terms of the crosstalk and the bandwidth will be achieved if the separation between the waveguides is increased, but it will be on the expense of the device length and the fabrication process. So there is a contradiction between the device length and the obtained bandwidth and crosstalk.



(a)



(b)

Figure 8 Variation of (a)  $P_{\text{out}}$  and (b)  $P_{\text{max}}$  with the wavelength at different  $W_1$  values

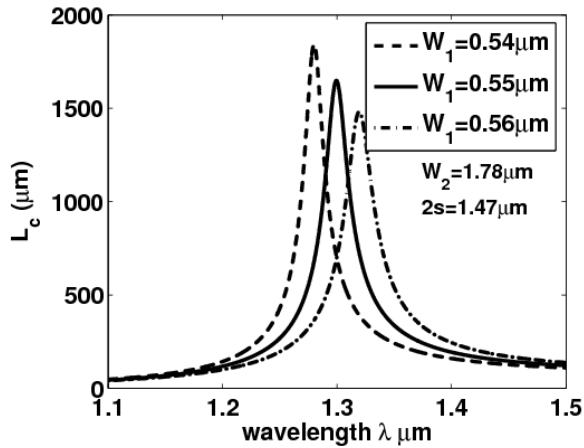


Figure 9 Variation of  $L_c$  with the wavelength at different  $W_1$  values

It should also be noted that the device temperature was kept at the room temperature 300K and the material of the reported structure has high stability at room temperature [17,22]. The variation of the refractive indexes  $n_1$  and  $n_2$  for the two guiding layers and the variation of the refractive index  $n_c$  of InP in the cladding and separation regions with the temperature [17,23] is shown in Fig. 10. It is revealed from this figure that the temperature has a negligible effect on the refractive indices  $n_1$ ,  $n_2$  and  $n_c$ . Therefore, the temperature variation around room temperature  $\pm 20K$  has a negligible effect on the output power and the coupling length of the suggested structure as shown in Fig. 11.

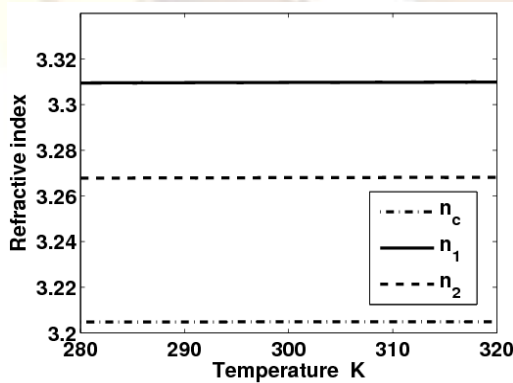


Figure 10 Variation of the refractive index with the temperature

All the performed simulations rely on achieving the phase matching between the waveguides modes. If the matching between the waveguides modes is lost, the efficiency of the power transfer at the operating wavelength of  $1.3\mu m$  will be decreased and no coupling between the waveguides modes can be achieved. Grating-assisted couplers [24], on the other hand, may achieve power coupling between two guided modes that are originally not

phase matched. But there are some limitations, for example, the grating perturbation such as the grating height and the grating width, must be small. Also, the index differences among different media must be small [12]. In the next section, a novel design of multiple stages of non-identical uniform directional coupler is introduced and analyzed by CMT. The objective of this design is to achieve the coupling between the waveguides modes which are originally not phase matched.

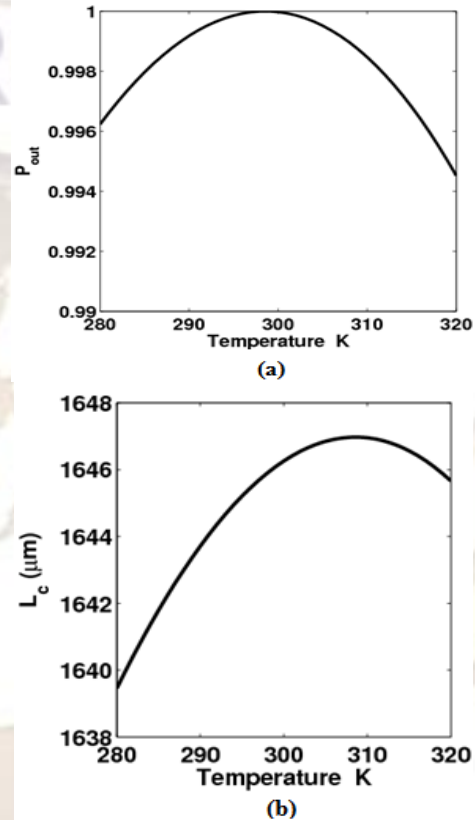


Figure 11 Variation of the (a) output power and (b) coupling length with the temperature.

#### 4. Design of Cascaded Structure of Non-Identical Directional Coupler

Figure 12 shows cross section of the proposed cascaded structure of non-identical directional coupler. The guiding media are isotropic, linear, and lossless. The widths  $W_1$  and  $W_2$  for each stage represent the width of the upper waveguide and the lower waveguide, respectively as shown from Fig. 1. In addition,  $2s_i$  represents the separation of the  $i^{th}$  stage where  $2s_{i+1}$  value is less than that of the  $2s_i$ . The device is designed to operate at  $\lambda=1.3\mu m$  and the length of each stage is fixed at its coupling length  $L_{Ci}$  and the device length is the summation of the individual coupling length of each stage.

$$L_C = \sum_{i=1}^k L_{Ci} \quad (11)$$

where,  $k$  represents the number of the cascaded stages.

The waveguides of the proposed design consist of  $\text{In}_{1-x}\text{Ga}_x\text{As}_y\text{P}_{1-y}$  material, for the guiding layers, with arsenic fractions ( $y$ ) of 0.25 for the first waveguide and 0.15 for the second waveguide. In addition, InP material is used for the cladding and separation layers.

A single section of the reported structure is first analyzed. In this case, the structure will be a conventional directional coupler as shown in Fig. 1. The structure parameters are taken as  $n_1=3.30970$ ,  $n_2=3.26799$ , and  $n_c=3.20483$ . In this investigation, only one waveguide is excited so that the input power is lunched to the first waveguide and the output power is the power of the second waveguide. In addition, the length of the stage is fixed to its coupling length  $L_c$ . Moreover,  $W_1$  and  $W_2$  are chosen in such a way that the waveguides modes are initially not matched. In this study,  $W_1$  and  $W_2$  are fixed to  $0.35 \mu\text{m}$  and  $1.78 \mu\text{m}$ , respectively. If the separation  $2s$  equals to  $0.7 \mu\text{m}$ , it is found that there is no coupling between the waveguides modes as shown in Fig. 13. It is also evident from this figure that the maximum value of the output power is increased by decreasing the separation  $2s$  to  $0.2 \mu\text{m}$ . However, the crosstalk will be increased to  $-2.0756 \text{ dB}$ . In addition, the value of  $2s$  can not be smaller than  $0.2 \mu\text{m}$  because it is not preferred for the coupled-mode analysis to use small separation values. In this case, exact composite modes of the parallel waveguides should be used as the basis for the trial solution [12,25].

In order to enhance the coupling efficiency without affecting on the accuracy of the results, cascaded stages of different separation values is used. The separation between the two waveguides decreases along the stages as shown in Fig. 12. For each stage,  $n_1=3.30970$ ,  $n_2=3.26799$ , and  $n_c=3.20483$ , at the operating wavelength  $\lambda=1.3 \mu\text{m}$ .

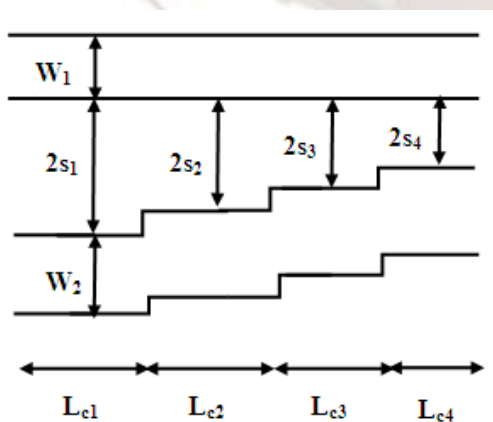


Figure 12 Schematic diagram of the cascaded structure of non-identical directional coupler

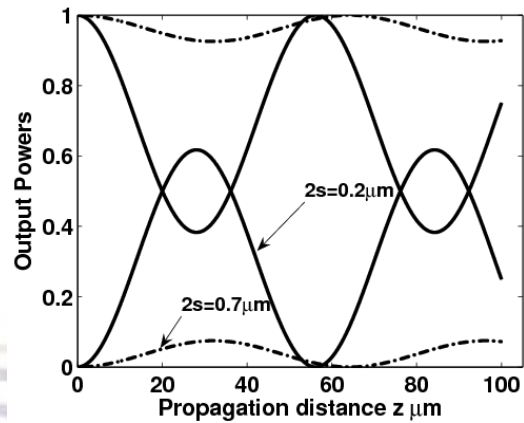


Figure 13 Variation of the output powers as a function of the propagation distance. The solid curves represent  $2s=0.2 \mu\text{m}$  while the dashed-dotted curves indicate  $2s=0.7 \mu\text{m}$ .

In this study, the separation of the first stage is fixed to  $2s_1=0.7 \mu\text{m}$  and  $\Delta s=2s_{i+1}-2s_i=0.1 \mu\text{m}$ . The variation in the output power of four cascaded stages structure as a function of propagation distance is shown in Fig. 14(a). It is observed from this figure that the coupling occurs after four cascaded stages with a device length of  $129.855 \mu\text{m}$ . In this case, the reported crosstalk and bandwidth are equal to  $-19.66 \text{ dB}$  and  $352 \text{ nm}$ , respectively. Next, If the separation of the first stage is fixed to  $2s_1=0.7 \mu\text{m}$  and  $\Delta s=2s_{i+1}-2s_i=0.05 \mu\text{m}$ , the variation in the output power of five cascaded structure as a function of propagation distance is shown in Fig. 14(b). In this case, the coupling occurs after five cascaded stages with crosstalk of  $-21.25 \text{ dB}$ , device length of  $161.304 \mu\text{m}$  and bandwidth of  $320 \text{ nm}$ .

The effects of the separations  $2s_1$  value and separation difference  $\Delta s_i$  on the crosstalk (CT), the total device length ( $L_c$ ) and the bandwidth (BW) are also studied and the results are reported in table 1. It is noticed from this table that there is a tradeoff between the total device length and the bandwidth.

Table 1 The device length ( $L_c$ ), crosstalk (CT) and bandwidth (BW) for different  $2s_1$  and  $\Delta s$  values.

$2s$ ( $\mu\text{m}$ )	$\Delta s$ ( $\mu\text{m}$ )	No. of stages	$L_c$ ( $\mu\text{m}$ )	CT (dB)	BW (nm)
1	0.2	5	171.54	-38.38	340
	0.1	7	230.52	-20.7	330
	0.05	8	259.28	-20.77	270
0.7	0.25	3	100.34	-16.6	480
	0.1	4	129.85	-19.66	352
	0.05	5	161.30	-21.25	320
0.5	0.1	3	95.39	-24.52	492
	0.05	3	94.99	-19.97	418

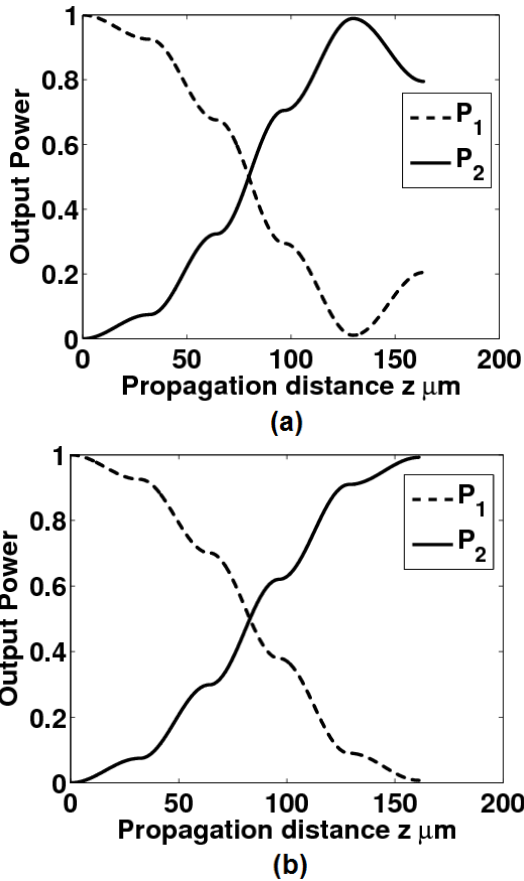


Figure 14 The output power of the cascaded structure of non-identical directional coupler (a)  $2s_1=0.7\mu\text{m}$  and  $\Delta s=2s_{i+1}-2s_i=0.1\mu\text{m}$ , (b)  $2s_1=0.7\mu\text{m}$  and  $\Delta s=2s_{i+1}-2s_i=0.05\mu\text{m}$ .

The single stage uniform coupler does not offer complete power transfer from one waveguide to the other waveguide if the waveguides modes are not originally phase matched. In addition, the coupling efficiency can be increased if the separation between the waveguides decreased. However, it will not be more than 60% as shown in Fig.13. Moreover, the proposed cascaded structure can exhibit low crosstalk up to  $-38.38$  dB for a device length of  $171.54$   $\mu\text{m}$  with  $\Delta s=0.2$   $\mu\text{m}$  and  $2s_1=1.0$   $\mu\text{m}$ . On the other hand, the single section conventional uniform directional coupler with the same structure parameters does not achieve coupling between the two waveguides. Therefore,  $W_1$  is taken as  $0.55$   $\mu\text{m}$  to achieve coupling between the waveguides modes which offer crosstalk of  $-34.9$  dB, device length of  $1646.26$   $\mu\text{m}$  and bandwidth of  $14.8$  nm. As a result, the device length of the cascaded structure will be much shorter than that of the conventional uniform directional coupler. In addition, the cascaded structure overcomes the sensitivity of the conventional directional coupler. However the bandwidth of the cascaded structure is larger than that of the conventional uniform directional coupler. The response of the cascaded structure with  $2s_1=1.0$   $\mu\text{m}$ ,  $\Delta s=0.2$   $\mu\text{m}$  is shown in Fig.

15. In order to decrease the bandwidth, the same structure parameters can be used with  $n_1=3.30970$ ,  $n_2=3.26799$ , and  $n_c=3.20483$  while  $W_1$  and  $W_2$  are taken as  $0.55$   $\mu\text{m}$  and  $1.5$   $\mu\text{m}$ . In this case, if the separation of the first stage is fixed to  $1.0$   $\mu\text{m}$  and  $\Delta s=0.1$   $\mu\text{m}$ , the coupling occurs with crosstalk of  $-21.16$  dB and bandwidth of  $180$  nm. However, the device length will be equal to  $1038.654$   $\mu\text{m}$ . It should be noted that the device length is still less than that of the conventional directional coupler.

In this study, the device temperature was kept at the room temperature  $300\text{K}$  and the material of the reported structure has high stability at room temperature [17,19]. The variation of the refractive indexes  $n_1$  and  $n_2$  for the two guiding layers and the variation of the refractive index  $n_c$  of InP in the cladding and separation regions with the temperature [17,23] is shown in Fig. 10. It is revealed from this figure that the temperature has a negligible effect on the refractive indices  $n_1$ ,  $n_2$  and  $n_c$ . Therefore, the temperature variation around room temperature  $\pm 20\text{K}$  has a negligible effect on the output power of the suggested structure of length  $171.54$   $\mu\text{m}$  with  $\Delta s=0.2$   $\mu\text{m}$  and  $2s_1=1.0$   $\mu\text{m}$  as shown in Fig. 16.

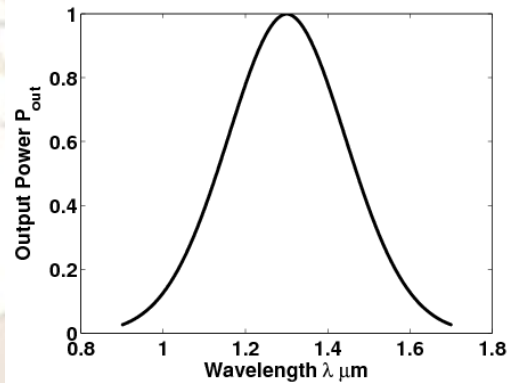


Figure 15 Variation of the output power with the wavelength for cascaded structure,  $2s_1=1$   $\mu\text{m}$ ,  $\Delta s=0.2$   $\mu\text{m}$

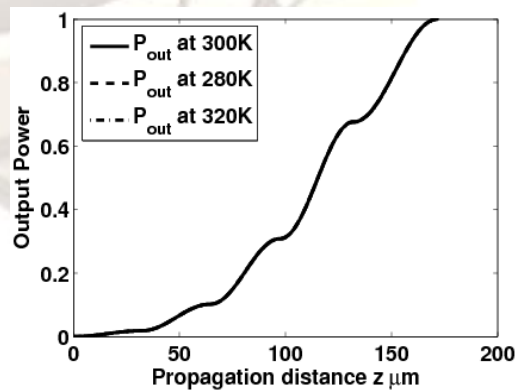


Figure 16 Variation of the output power with the temperature for cascaded structure,  $2s_1=1$   $\mu\text{m}$ ,  $\Delta s=0.2$   $\mu\text{m}$

## 5. CONCLUSION

A novel design of an optical wavelength filter of non-identical directional coupler have been presented and analyzed by CMT. The numerical results reveal that the proposed design offers complete power transfer at the resonance wavelength of 1.3  $\mu\text{m}$  over a coupling length of 1646.26  $\mu\text{m}$ . The reported bandwidth is 14.8 nm which can be further improved by increasing the separation between the waveguides. However, this will be on the expense of increasing the coupling length and the complexity of the fabrication process. The effects of the structure parameters on the design performance are reported. In addition, a novel design of cascaded structure of non-identical directional coupler is introduced and analyzed. The suggested cascaded structure offers a device length of 171.54  $\mu\text{m}$  which is shorter than that of the conventional coupler with nearly equal crosstalk values. Moreover, the cascaded structure overcomes the sensitivity of the conventional directional coupler to the structure geometrical parameters.

## REFERENCES

- [1] J. P. Donnelly, L. A. Molter, and H. A. Haus, The extinction ratio in optical two guide coupler A3 switches, *IEEE J. Quantum Electron.*, 25, 1989, 924-932.
- [2] R. R. A. Syms, and R. G. Peall, The digital optical switch: analogous directional coupler devices, *Opt. Commun.*, 68, 1989, 235-238.
- [3] H. Kogelnik, and R. V. Schmidt, Switched directional couplers with alternating AD, *IEEE J. Q. Electron.*, QE-12, 1976, 396-401.
- [4] B. Pucel, L. Riviere, and J. L. Bihan, New model for the active directional coupler, *J. Lightwave Technol.*, 14, 1996, 1501-1506.
- [5] M. L. Farewell, W. S. C. Chang, and J. H. Schaffner, A directional coupler modulator with improved linearing (operating up to 1 GHz). In Broadband Analog and Digital Optoelectron, *Digest of LEOS Summer Topical Meeting, WA3*, 1993, 8-9.
- [6] W. B. Bridges, F. T. Sheehy, and J. H. Schaffner, Wave-coupled electro-optic modulators for microwave and millimeter wave modulation, *IEEE Photon. Technol. Lett.*, 3, 1991, 133-135.
- [7] R. C. Alfemess, L. L. Buhi, U. Koren, B. I. Miller, M. Young, and L. Koch, in *Tech. Digest OFC'91, ThE32* 1991.
- [8] H. Sakata, and S. Takeuchi, *IEEE Photon. Techn. Lett.*, 3, 1991, 990.
- [9] A. B. Fallahkhair, K. S. Li, and T. E. Murphy, Vector Finite Difference Modesolver for Anisotropic Dielectric Waveguides, *J. Lightwave Technol.*, 26 (11), 2008, 1423-1431.
- [10] S. S. A. Obayya, B. M. A. Rahman, K. T. V. Grattan, and H. A. El-Mikati, Full vectorial finite-element-based imaginary distance beam propagation solution of complex modes in optical waveguides, *J. Lightwave Technol.*, 20, 2002, 1054-1060.
- [11] W. P. Huang, and C. L. Xu, Simulation of three-dimensional optical waveguides by a full-vector beam propagation method, *IEEE journal of quantum electronics*, 29, No10, 1993, 2639-2649.
- [12] Wei-Ping Huang, Coupled-mode theory for optical waveguides: an overview, *J. Opt. Soc. Am. A* 11, 1994, 963-983.
- [13] H. A. Haus, W. P. Huang, S. Kawakami, and N. A. Whitaker, Coupled- mode theory of optical waveguides. *J. Lightwave Technol.*, LT-5, 1987, 16-23.
- [14] A. Hardy, and W. Streifer, Coupled modes of multiwaveguide systems and paired arrays, *J. Lightwave Technol.*, LT-4, 1986, 90-99.
- [15] W. Streifer, M. Osinski, and A. Hardy, Reformulation of coupled-mode theory of multiwaveguide systems, *J. Lightwave Technol.*, LT-5, 1987, 1-4.
- [16] T. Tamir, ed. *Guided-Wave Optoelectronics* (Springer- Verlag, New York, 1988).
- [17] B. Broberg, and S. Lindgren, Refractive index of  $\text{In}_{1-x}\text{Ga}_x\text{As}_y\text{P}_{1-y}$  layers and InP in the transparent wavelength region, *J. Appl. Phys.*, 55, 1984, 3376-3381.
- [18] O. J. Glembocki, and H. Piller, *Indium Phosphide (InP)* (Handbook of Optical Constants of Solids, E. D. Palik, Ed. New York: Academic, 1985).
- [19] B. Broberg, S. Lindgren, and H. Jiang, A novel integrated optics wavelength filter in InGaAsP-InP, *J. Lightwave Technol.*, 4, 1986, 196-203.
- [20] H. F. Taylor, Frequency selectivity coupling in parallel dielectric waveguides, *Opt. Commun.*, 8, 1973, 421-425.
- [21] T. Wongcharoen, B. M. Azizur Rahman, and T. V. Kenneth, Accurate Characterization of Optical Filters with Two-Dimensional Confinement Technol, *J. Lightwave LT-5*, 1996, 2596 - 2603.
- [22] B. Rheinlander, et al, room temperature polarization bistability in 1.3 $\mu\text{m}$  InGaAsP/InP ridge waveguide lasers, *Opt. Commun.*, 80, 1991, 259-261.
- [23] E. Herbert, and Li, *Physica E*, 5, 2000, 215.
- [24] J. Hong, and W. P. Huang, Asymmetric power coupling in grating-assisted couplers, *IEE Proc-optoelectronics*, 142, 1995, 103-108.
- [25] D. Marcuse, Directional couplers made of nonidentical asymmetrical slabs. partII : grating-assisted couplers, *J. Lightwave Technol.* LT-5, 1987, 268-273.